Proceedings of the 14th International Symposium Ultrafast Phenomena in Semiconductors, Vilnius 2010

Efficient Terahertz Emission from InGaN/GaN Heterostructure

A. Reklaitis

Semiconductor Physics Institute, Centre for Physical Sciences and Technology
A. Goštauto 11, LT-01108 Vilnius, Lithuania

Terahertz emission from the freestanding InGaN/GaN heterostructure illuminated by femtosecond optical pulse is considered using Monte Carlo simulations. The results of Monte Carlo simulations show that the power of terahertz emission from InGaN/GaN heterostructure exceeds the power of the emission from InN surface by one order of magnitude.

PACS: 42.72.Ai, 73.20.Mf, 75.70.–i, 78.20.Bh, 78.47.−p

1. Introduction

Pulsed terahertz (THz) radiation from semiconductors excited by femtosecond laser has been studied extensively in the recent years. The two main methods [1] are used to generate the broadband THz radiation. The methods are based on THz emission from the biased photoconductive switches and on THz emission from the surface of freestanding semiconductors. Multiple mechanisms are responsible for the THz emission from the freestanding semiconductor surface including nonlinear optical rectification, photocurrent induced by the surface-field, photocurrent induced by the built-in field in p–i–n structures, and by photocurrent induced photo-Dember effect. However, the intensity of THz emission from the surface of freestanding semiconductors still is very low.

The analysis [2] of the transient dynamics of photoexcited carriers shows that the surface and contactless p–i–n THz emitters have serious deficiencies that significantly reduce the intensity of THz radiation. First, only a minor part of the excited carriers contributes to the transient current if the inverse absorption coefficient exceeds the surface depletion width or the i-layer thickness of the p–i–n structure. In this case, the major part of carriers is created in the region where the built-in electric field is screened by the extrinsic carriers. Second, the plasma frequency of photocarriers is position-dependent due to the exponential decay of the created carrier density. As a result, the transient response of the created carriers is incoherent in different regions of the structure because the frequency of current oscillations is position-dependent. Therefore, the amplitude of oscillations of the resulting current is significantly reduced by the interference effects.

To overcome such deficiencies of THz emitters, the novel δ-doped GaAs/AlGaAs heterostructure is suggested in [2]. It is shown in [2] that THz energy radiated from the freestanding semiconductors is significantly enhanced when the above noted deficiencies are eliminated. It is obtained from Monte Carlo simulations that the efficiency of THz emission from the δ-doped GaAs/AlGaAs heterostructure exceeds the efficiency of THz emission from the homogeneous GaAs by two orders of magnitude.

In the present work, the basic ideas suggested in [2] are used to design THz emitters based on InGaN/GaN heterostructures. The pulsed THz emission from the InGaN/GaN heterostructures is studied using Monte Carlo simulations [2, 3] of the transient dynamics of photoexcited electron–hole plasma. The InGaN/GaN heterostructures appear to be very suitable for the development of highly efficient THz emitters. High electron mobility in the optically active InGaN layers provides a large amplitude of the transient current. The offsets of the conduction and valence bands at the InGaN/GaN heterointerfaces are sufficiently high to ensure the perfect confinement of the excited carriers inside the InGaN layers. In addition to the basic ideas of [2], the polarization charges at the InGaN/GaN interfaces are employed in the design of the appropriate potential profile in the InGaN/GaN heterostructures for the efficient THz emission.

2. Model of InGaN/GaN heterostructure

The parameters of the conduction band and electron scattering for InGaN/GaN heterostructures are taken from the set of parameters listed in [4] for InN/GaN heterostructure. The linear interpolation between InN and GaN is used for the evaluation of parameters for $In_{1-x}Ga_xN$/GaN heterostructures. The material parameters for valence band of InGaN/GaN heterostructures are taken from [5]. The surface Fermi level pinned at 1.6 eV above the valence band maximum [6, 7] is accepted in the simulations.

The simulations of the optically excited electron–hole plasma are carried out by ensemble Monte Carlo method as described in [2, 3]. The simulations are started from the thermally equilibrium distribution of carriers. The duration of the optical pulse τ_F is set to 100 fs. The performance of the InGaN/GaN THz emitter is studied for the 800 nm wavelength of the optical excitation. The absorption coefficients of the $In_{1-x}Ga_xN$ layers for this wavelength are evaluated from the absorption spectrum of InN [8] using the linear extrapolation to the $In_{1-x}Ga_xN$ band-gap. The estimated absorption coefficient of $In_{1-x}Ga_xN$ ranges between 7×10^4 cm^{-1} and 2×10^4 cm^{-1} for x ranging between $x = 0$ and $x = 0.28$, respectively. The absorption coefficient $\alpha = 2.7 \times 10^4$ cm^{-1} is taken for $In_{0.75}Ga_{0.25}N$.

Several structures of the $In_{1-x}Ga_xN$/GaN THz emitter have been investigated for the best performance. The optimized structure is composed from four periods of narrow band-gap optically-active n-$In_{0.75}Ga_{0.25}N$ layers doped to 10^{17} cm^{-3} and from wide band-gap n-GaN barriers doped to 2×10^{17} cm^{-3}. The thickness L_i of each InGaN layer is taken as 110 nm. The thickness of GaN barriers is taken as 20 nm. The simulated structure is completed by the substrate layer of 150 nm doped to 10^{17} cm^{-3} $n-In_{0.75}Ga_{0.25}N$. The optimized structure is shown in Table.

TABLE

Schematic diagram of the $In_{1-x}Ga_xN$/GaN THz emitter.

Layer	Thickness [nm]	Doping [cm^{-3}]
n-$In_{0.75}Ga_{0.25}N$	110	1×10^{17}
n-GaN barrier	20	2×10^{17}
n-$In_{0.75}Ga_{0.25}N$	110	1×10^{17}
n-GaN barrier	20	2×10^{17}
n-$In_{0.75}Ga_{0.25}N$	110	1×10^{17}
n-GaN barrier	20	2×10^{17}
n-InN	110	1×10^{17}
n-GaN barrier	20	2×10^{17}
n-$In_{0.75}Ga_{0.25}N$ (substrate)	150	1×10^{17}

3. Results and discussion

The calculated equilibrium potential profile and carrier distribution in the four-period InGaN/GaN emitter are presented in Fig. 1. The polarization charges at InGaN/GaN interfaces provide a high built-in electric field in the optically active InGaN layers. The average built-in electric field in the InGaN layers is close to ε_g/eL_i, where ε_g is the band-gap energy and e is the electron charge. The strength of the average built-in electric field reaches 110 kV/cm in the InGaN layers. The high built-in electric field ensures a fast acceleration of photoexcited carriers, and thus, high amplitude of transient photocurrent.

The comparison of the transient photocurrent in n-InN and n-InGaN/GaN heterostructure after the optical pulse duration of 100 fs is shown in Fig. 2. The transient photocurrent in homogeneous InN is induced by the photo-Dember effect due to downward band bending at InN surface [9]. Contrary to that, the photocurrent in InGaN/GaN heterostructure is induced by the strong polarization charges at the InGaN/GaN heterointerfaces, and the photo-Dember effect is completely suppressed. Therefore, the transient photocurrents in InN and InGaN/GaN are of opposite directions. The homogeneous InN is identified as one of the most efficient emitters of pulsed THz radiation [9]. The results presented in Fig. 2 show that the efficiency of the heterostructure InGaN/GaN emitter essentially exceeds the efficiency of the InN emitter. The amplitude of the transient photocurrent in the InGaN/GaN heterostructure is approximately five times higher than the transient photocurrent in the InN.

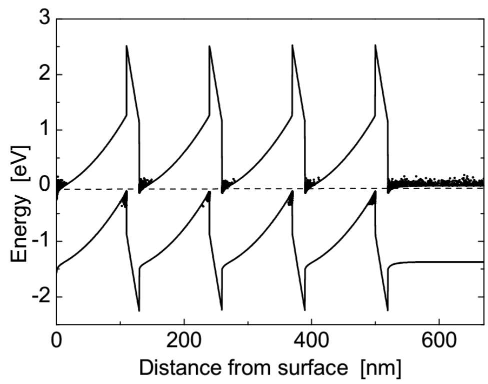

Fig. 1. Equilibrium potential profile (conduction and valence band edges) in the InGaN/GaN emitter (solid curves) and electron and hole kinetic energies (points) before photoexcitation. The dashed line shows the Fermi level.

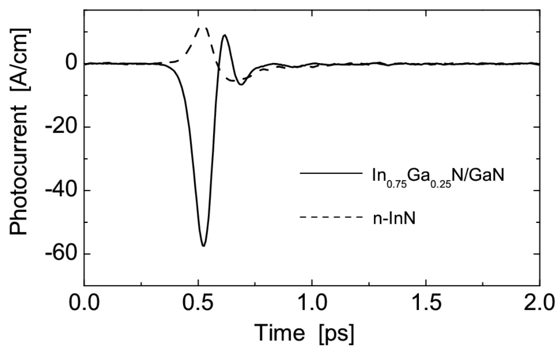

Fig. 2. Waveforms of the transient current in the InGaN/GaN emitter (solid curve) and in the n-InN doped to 10^{17} cm^{-3} (dashed curve). The optical fluence is 10 μJ/cm^2. The peak of the optical pulse intensity is at $t = 0.5$ ps, and τ_F is set to 100 fs.

The energy and spectrum of THz radiation are obtained from the simulated transient current of photoexcited carriers. The time-dependent THz power $P(t)$ radiated in all directions by the electric dipole moment $\boldsymbol{D}(t)$ and the first derivative of the dipole moment are evaluated as [2]:

$$P(t) = \frac{1}{6\pi\varepsilon c^3}\left(\frac{d^2\boldsymbol{D}(t)}{dt^2}\right)^2 \tag{1}$$

and

$$\frac{\mathrm{d}\boldsymbol{D}(t)}{\mathrm{d}t} = \int \boldsymbol{j}(\boldsymbol{r},t)\,\mathrm{d}V\,, \tag{2}$$

where ε is the vacuum permittivity, c is the speed of light, $\boldsymbol{j}(\boldsymbol{r},t)$ is the current density of electrons and holes, and the integration is taken over the volume V of the photoexcitation. The total THz energy radiated in all directions is obtained by the integration of $P(t)$ over the duration of transient evolution of photoexcited carriers. The spectrum of radiation is found from the Fourier analysis of $P(t)$. The calculated spectra of radiation are shown in Fig. 3.

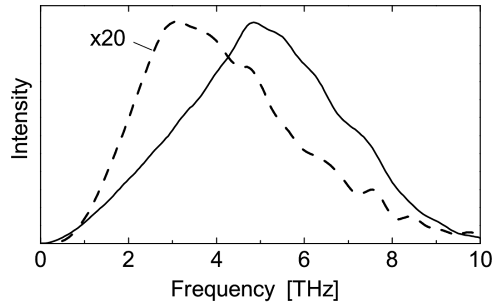

Fig. 3. Spectra of THz emission from InGaN/GaN emitter (solid curve) and from n-InN (dashed curve). The optical fluence is 10 μJ/cm^2, and τ_F is 100 fs.

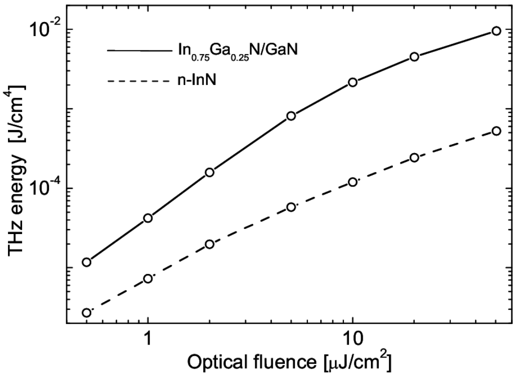

Fig. 4. Radiated THz energy as a function of the optical fluence. The solid and dashed curves present the energy radiated from the four-period InGaN/GaN heterostructure and from n-InN doped to 10^{17} cm^{-3}, respectively. The pulse duration τ_F is set to 100 fs.

The comparison of the intensity of THz emission from the homogeneous n-InN and from the InGaN/GaN heterostructure is presented in Fig. 4. Due to downward bend bending, THz emission from the InN is caused by the relatively weak photo-Dember effect [9]. Contrary to that, THz emission from the $In_{1-x}Ga_xN$/GaN heterostructure is induced by the strong built-in electric field. Therefore, the intensity of THz emission from the $In_{1-x}Ga_xN$/GaN heterostructure essentially exceeds the intensity of THz emission from the InN surface. The dependence of intensity of THz emission from the $In_{1-x}Ga_xN$/GaN heterostructure on the optical fluence I_0 is near-proportional to I_0^2 in the range $I_0 \leq 10\ \mu$J/cm^2.

According to the hydrodynamic theory [2] of heterostructure emitters, the emitted THz energy is proportional to the squared built-in electric field and inversely proportional to the momentum relaxation rate γ. The momentum relaxation rate in InN is evaluated using Monte Carlo method suggested in [10]. It is found that the momentum relaxation rate of photoelectrons in $In_{0.75}Ga_{0.25}N$ excited by 800 nm optical pulse is 6×10^{12} s^{-1} which is close to momentum relaxation rate 7×10^{12} s^{-1} in GaAs [2]. Therefore, one could expect that the efficiency of the InGaN/GaN heterostructure emitter should be of the same order as the GaAs/AlGaAs emitter considered in [2]. The results of Monte Carlo simulations of InGaN/GaN and GaAs/AlGaAs THz emitters confirm this expectation. Moreover, the InGaN/GaN heterostructures have a significant advantage in the development of efficient THz emitters because the role of δ-doped layers in GaAs/AlGaAs emitter is played by the inherent polarization charges in InGaN/GaN emitter.

4. Conclusions

In conclusion, the efficient InGaN/GaN emitter of pulsed THz radiation is proposed and investigated using Monte Carlo simulations. The THz energy emitted from the suggested InGaN/GaN emitter exceeds the energy of THz radiation from InN by one order of magnitude.

Acknowledgments

This work was supported by the Research Council of Lithuania under contract No. MIP-49/2010.

References

[1] *Terahertz Optoelectronics*, Ed. K. Sakai, Springer, Berlin 2005.

[2] A. Reklaitis, *Phys. Rev. B* **77**, 153309 (2008).

[3] A. Reklaitis, *Phys. Rev. B* **74**, 165305 (2006).

[4] A. Reklaitis, *J. Phys., Condens. Matter* **20**, 384202 (2008).

[5] I. Vurgaftman, J.R. Meyer, *J. Appl. Phys.* **94**, 3675 (2003).

[6] I. Mahboob, T.D. Veal, C.F. McConville, H. Lu, W.J. Schaff, *Phys. Rev. Lett.* **92**, 036804 (2004).

[7] I. Mahboob, T.D. Veal, L.F.J. Pipper, C.F. McConville, H. Lu, W.J. Schaff, J. Furthmüller, F. Bechstedt, *Phys. Rev. B* **69**, R201307 (2004).

[8] J. Wu, W. Walukiewicz, S.X. Li, R. Armitage, J.C. Ho, E.R. Weber, E.E. Haller, H. Lu, W.J. Schaff, A. Barcz, R. Jakiela, *Appl. Phys. Lett.* **84**, 2805 (2004).

[9] R. Ascazubi, I. Wilke, K. Denniston, H. Lu, W.J. Schaff, *Appl. Phys. Lett.* **84**, 4810 (2004).

[10] Yu. Pozhela, A. Reklaitis, *Fiz. Tekh. Poluprovodn. (S.-Petersburg)* **13**, 1127 (1979) [*Sov. Phys.-Semicond.* **13**, 660 (1979)].